Journal of Catalysis **191,** 326–331 (2000)
doi:10.1006/jcat.1999.2800, available online at http://www.idealibrary.com on IDEAL®

Catalytic and Sorption Studies Related to the *para* Selectivity in the Ethylbenzene Disproportionation over H-ZSM-5 Catalysts

N. Arsenova-Härtel,* H. Bludau,* R. Schumacher,† W. O. Haag,[1] H. G. Karge,*,[2] E. Brunner,‡ and U. Wild*

*Fritz Haber Institute of the Max Planck Society, Faradayweg 4-6, 14195 Berlin, Germany; †Schuit Institute of Catalysis, Faculty of Chemical Engineering, TU Eindhoven, P.O. Box 513, NL5600MB, Eindhoven, The Netherlands; and ‡Institute for Biophysics and Physical Biochemistry, University Regensburg, 93040 Regensburg, Germany

Received July 19, 1999; revised November 10, 1999; accepted November 12, 1999

Earlier kinetic investigations of ethylbenzene disproportionation over medium-pore zeolite catalysts revealed that the *para* selectivity for the diethylbenzenes produced increases strongly with crystal size. Two models for diethylbenzene isomerization have been offered as a possible explanation for the observed dependence: secondary isomerization on the external surface of the zeolite crystallites (I) and isomerization inside the zeolite pores combined with faster diffusion of *para*-diethylbenzene (II). The present paper describes additional investigations, aimed at obtaining evidence for one of these models. Thus, in a series of catalytic experiments the effect of the deactivation of the outer crystallite surface of H-ZSM-5 samples on the distribution of the diethylbenzene product was examined. Further, sorption of pure *para*-, *meta*-, and *ortho*-diethylbenzene from the gas phase over H-ZSM-5 was studied by means of *in situ* infrared spectroscopy. Both types of investigations provided evidence that diethylbenzene isomerization occurs in the interior of H-ZSM-5. Thus, the *para*-selective features of H-ZSM-5 reflect the interplay of catalytic reaction and mass transfer phenomena. It was additionally shown that *para*-diethylbenzene and *meta*-diethylbenzene are reversibly sorbed in H-ZSM-5 in contrast to the *ortho* isomer, which cannot enter the zeolite pore system in the temperature range examined (359–522 K).

Key Words: **H-ZSM-5-zeolite; *para* selectivity; ethylbenzene disproportionation; diethylbenzene isomerization; adsorption; IR spectroscopy.**

INTRODUCTION

The research on shape-selective formation of substituted aromatics over zeolite catalysts attracted significant interest in past years, from both academic and industrial institutions [e.g., cf. Refs. (1–12)]. The attention was focused mainly on H-ZSM-5 zeolite because of its unique combination of high activity, stability, and shape selectivity. Its ability to produce *para*-dialkylbenzenes in concentrations exceeding by far the equilibrium values measured in the absence of geometric constraints has led to the development and commercial use of several processes in the petroleum and petrochemical industry (13–16). This paper describes a series of catalytic and sorption experiments concerning the mechanism of *para* selectivity in the ethylbenzene (EB) disproportionation to benzene (B) and diethylbenzenes (DEBs) over H-ZSM-5 catalysts. The high yield of *p*-DEB is of interest because it is commercially used in the Parex process for separation of xylene isomers and as an intermediate in the production of *para*-divinylbenzene.

An earlier kinetic investigation of the disproportionation of EB over H-ZSM-5 zeolites showed that the reaction follows a consecutive path (17). Since essentially no *o*-DEB is produced over this zeolite, the reaction scheme can be approximated by the following equations:

$$2\text{EB} \leftrightarrow \text{B} + p\text{-DEB}, \quad [1]$$

$$p\text{-DEB} \leftrightarrow m\text{-DEB}. \quad [2]$$

It was shown (17) that the first step in EB disproportionation [1] occurs in the interior of the zeolite crystal without diffusion limitations, yielding essentially *p*-DEB as a primary product. The latter is converted in a secondary isomerization [2] mainly to *m*-DEB. A strong influence of crystal size on the product distribution was observed. Thus, the *p*-DEB content produced over the large crystals was significantly higher than that over the small crystals. In other words, the observed rate of isomerization increases with decreasing crystal size of the catalyst. This could be accounted for by two models.

Model I. The isomerization of *p*-DEB to the bulky *m*-DEB is sterically restricted to active sites on the outer crystallite surface which is inversely proportional to the crystallite radius, r (18–20).

Model II. The isomerization occurs on active sites both on the external surface and in the interior of the zeolite. The slim *para* isomer, however, diffuses more rapidly toward the gas phase than the bulky *m*-DEB (21). Thus, the isomerization becomes diffusion-limited with increasing crystal size (1–7). For severe mass transfer limitations (Thiele modulus, $\varphi > 3$) the relationship between the

[1] Deceased.

[2] To whom correspondence should be addressed.

0021-9517/00 $35.00

observed isomerization rate constant (k_i^{obs}) and the intrinsic rate constant (k_i^0) is given [cf. Refs. (22, 23)] by the Thiele-type equation

$$k_i^{obs} = \frac{\sqrt{k_i^0 D}}{r}, \qquad [3]$$

where D is the diffusivity of the slow reactant, i.e., *m*-DEB, when the product *o*-DEB can be neglected (see above).

As apparent from the discussion above, for both models the rate of isomerization is inversely proportional to the crystal radius. Thus, it is impossible to distinguish between them on the base of kinetic results. This study describes a series of catalytic and sorption experiments aimed at obtaining evidence for one of the two models.

EXPERIMENTAL

Samples

Two specimens of H-ZSM-5, which have crystal dimensions in the direction of the straight channels (main diffusion way) of ca. 0.02–0.05 and 1–3 μm, and are designated below as "small" (S) and "large" (L), respectively, were obtained from Mobil Corporation. Crystal size was determined by scanning electron % microscopy (SEM). ^{29}Si magic-angle spinning (MAS) NMR and ^{27}Al MAS NMR measurements showed that both zeolite samples are essentially free of nonframework aluminum and their n_{Si}/n_{Al} ratio was 35. XPS investigations yielded similar n_{Si}/n_{Al} ratios for the crystallite surface, viz., 39 and 37 for samples S and L, respectively. Another H-ZSM-5 sample was synthesized by H. K. Beyer, Budapest, Hungary. It was round, with a mean crystallite diameter of 2 μm and a bulk n_{Si}/n_{Al} ratio of 34 as determined by atomic absorption spectrophotometry. Zeolite Na-Y with an n_{Si}/n_{Al} ratio of 2.5 was obtained from Union Carbide.

Oxalic Acid Treatment of the Zeolite Catalysts

H-ZSM-5 samples S and L were suspended in a 2 M aqueous oxalic acid solution. The suspension was intensely mixed by the flow of an inert gas at 345 K. The duration of the treatment was either 1.5 or 3.0 h. After settling and decantation, the zeolite had washed with distilled water until the wash water had pH $\sim$ 7, and dried for 10 h at 373 K. Afterward the samples were heated in a flow of dry synthetic air (80 ml/min) at the rate of 2 K/min up to 413 K and then at 3 K/min up to 643 K and finally calcined for 3 h at 643 K.

Spectroscopic Investigations

NMR investigations were carried out on a Bruker MSL 500 spectrometer. The n_{Si}/n_{Al} framework ratios were determined by ^{29}Si MAS NMR (24). ^{1}H MAS NMR spectra were measured on sealed samples prepared as previously described (25) at 180 K with a sample spinning rate of 3.8 kHz. XPS measurements were carried out in a modified LHS-12-MCD system in a UHV chamber without heating, the zeolite samples having been prepared as thin continuous films. Al 2*p*, Si 2*p*, and O 1*s* lines (74.4, 102.9, and 532.0 eV BE, respectively) were used for composition determination. Quantitative XPS data analysis was performed by subtracting stepped backgrounds and using empirical cross sections (26).

Catalytic Experiments

The disproportionation of EB was applied as a test reaction to estimate the activity and *para* selectivity of the H-ZSM-5 catalysts under study. The zeolite samples were pressed binder-free, crushed, and sieved. A sieve fraction of 0.2–0.4 mm was used. The catalyst was diluted with washed sand (Merck, Seesand p.a.) 0.1–0.3 mm in particle size. The EB (purchased from Merck, "for synthesis" grade) was purified of polar contamination by passage through calcined Al_2O_3. Catalytic experiments were carried out in a fixed-bed flow reactor as previously described (27). Prior to the reaction, the catalyst was activated *in situ* in a flow of dry helium. The feed was introduced by flowing dry carrier gas through a saturator containing freshly purified EB kept at 298 K to obtain a partial pressure of EB of 1.33 kPa. The reaction temperature was varied between 498 and 565 K.

Sorption Kinetic Experiments

Since Olson and Haag (3) have demonstrated that the diffusion coefficient of *o*-xylene in H-ZSM-5 zeolites can be used as a criterion for the mass transfer in this zeolite, sorption kinetic measurements with *o*-xylene were carried out in an apparatus of constant-volume/variable-pressure type (21, 28). Prior to the sorption experiments, the sorbent was heated in high vacuum (ca. 10^{-5} Pa) at a heating rate never exceeding 2 K/min up to 675 K and held at this temperature for 4 h. The *o*-xylene (purchased from Fluka, "spectroscopic" grade) was freed of polar contamination in the same way as EB used in the catalytic experiments (see above). Five freeze–pump–thaw cycles were conducted for further purification of the sorbate. Sorption kinetic experiments were carried out at 395 K. The temperature in the gas phase was held constant to about $\pm$0.5 K, and that of the zeolite sample to about $\pm$0.1 K. A single sorbate pressure jump of ca. 46 Pa was applied over the sorbent in all experiments. Diffusion coefficients were determined by fitting the experimental data by an analytical solution of Fick's second law under appropriate boundary conditions (28).

In Situ Infrared Spectroscopic Study of the Sorption of the DEB Isomers over H-ZSM-5

The isomers *p*-, *m*-, and *o*-DEB were purchased from Merck and were of "synthesis grade." All substances were

purified of polar impurities by passage through calcined Al_2O_3.

The pure DEB isomers were sorbed from the gas phase over zeolite samples with crystallite diameters of 0.02–0.05 and of 2 μm. The sorbent was pressed into self-supporting wafers, placed into the sample holder, and introduced into the furnace of the IR cell. [For equipment details see Ref. (29).] The zeolite was heated in the evacuated system (5 K/min) to 675 K and degassed for 2 h (10^{-6} Pa). Subsequently, a well-defined quantity of sorbate from a dosing reservoir was exposed to the sample. The sorption process was monitored by following the change in sorbate pressure and in the IR spectra of the zeolite sorbent. The experiments were conducted at 359 and 522 K, whereas the equilibrium pressure of the sorbate was varied between 12 and 61 Pa.

Since the bands of the C–H stretching vibrations are very similar for all the aromatic compounds under study, the characteristic bands of the ring vibrations were used for identification. The aromatic C–C stretching vibrations give rise to multiple bands in the region 1400–1650 cm^{-1}, whose position and intensity depend strongly on the type and location of the substituents in the benzene ring. The 1600 cm^{-1} vibrations involve mainly quadrant stretching of the C–C bonds. For 1,4-DEB, which has identical groups in *para* position, the quadrant stretching vibrations are infrared inactive. At variance, the 1,3-DEB isomer exhibits an intense doublet in the region of 1600 cm^{-1}. These two isomers differ also in the semicircle stretching vibrations of the carbon bonds in the 1500 cm^{-1} region. For *meta* substitution a band usually appears at 1510–1470 cm^{-1}. This band is generally 10–20 cm^{-1} higher for *para* isomers than for the other isomers and is clearly separated in the spectrum of the isomers (30).

RESULTS AND DISCUSSION

1. *Selective Deactivation of the External Crystallite Surface*

To elucidate the role of the acidic sites of the external surface in DEB isomerization, the crystallite surface was selectively dealuminated and, thus, deactivated. Apelian (31) has shown that oxalic acid hydrolyzes aluminum from the zeolite framework and chelates with the Al^{3+} ions to aluminum oxalates. Being larger than the cross sections of the channels of H-ZSM-5 zeolites, the chelate complexes, $[Al(^{-}OOC–COOH)_3]$, cannot form and diffuse in their channel system. As a result the external crystallite surface is selectively dealuminated (31–33). H-ZSM-5 samples S and L, which exhibit essentially the same interior and surface n_{Si}/n_{Al} ratios but differ in size by a factor of ca. 50, were treated with 2 M oxalic acid over 1.5 and 3 h. If the isomerization of DEB occurred only on the crystallite surface (model I), it is to be expected that deactivation of the latter would result in enhancement of the *para* selectivity of both catalysts. This effect, however, should be particularly pronounced for the sample with the smaller crystals.

TABLE 1

Effect of the Duration of the Oxalic Acid Treatment of H-ZSM-5 Zeolites on the Aluminum Concentration on the Crystallite Surface, $(Al/Al + Si)_{sf} \cdot 100$ (%)

Zeolite	d μm	Duration of treatment 0 h	1.5 h	3 h
			$(Al/Al + Si)_{sf} \cdot 100$ (%)	
H-ZSM-5	1–3	0.26	0.18	0.18
H-ZSM-5	0.02–0.05	0.25	0.17	0.17

The chemical surface composition of the two H-ZSM-5 specimens was studied by means of XPS prior to and after oxalic acid treatment. The data are summarized in Table 1. One should bear in mind that the element concentrations estimated via this method represent average values for a shell of several atom layers. Therefore, the aluminum concentrations of the uppermost surface layers of the dealuminated samples were most probably lower than the values given in Table 1. As is apparent from the data, oxalic acid treatment reduced the aluminum concentration, $(Al/Al + Si)_{sf}$, and, consequently, the concentration of Brønsted acid sites on the crystallite surface. The decreases in aluminum concentration for the two samples of different crystal size were essentially the same and did not depend on the duration of the treatment (1.5 h vs 3 h). If the isomerization of DEB took place only on the outer surface, then an increase in the *para* content of the product after acid modification of both catalysts is to be expected.

However, irrespective of which of the two isomerization models applies, there are a number of catalyst features besides the external acidity that strongly influence *para* selectivity. Thus, as follows from the reaction scheme (Eqs. [1] and [2]), the *p*-DEB content of the product depends on the ratio of the rates of the reactions in which *p*-DEB is produced (disproportionation) and consumed (isomerization). Hence, assessing the influence of oxalic acid treatment on the *para*-selective properties of the catalyst, modification of both the isomerization and the disproportionation activity should be taken into account. Furthermore, the *para* content of the product depends inversely on the crystal size of the catalyst according to both models I and II (see above). When model II is valid, possible changes in the diffusion coefficient (D) of the "slow reactant" should be considered (Eq. [3]). Therefore, in studying the influence of oxalic acid treatment on the *para* selectivity of H-ZSM-5 samples in the disproportionation of EB, not only the external acidity but also the above-mentioned parameters were examined.

Figure 1 provides electron microscope photographs of the catalyst with the larger crystals prior to and after treatment with the acid solution for 3 h. No evidence of a change

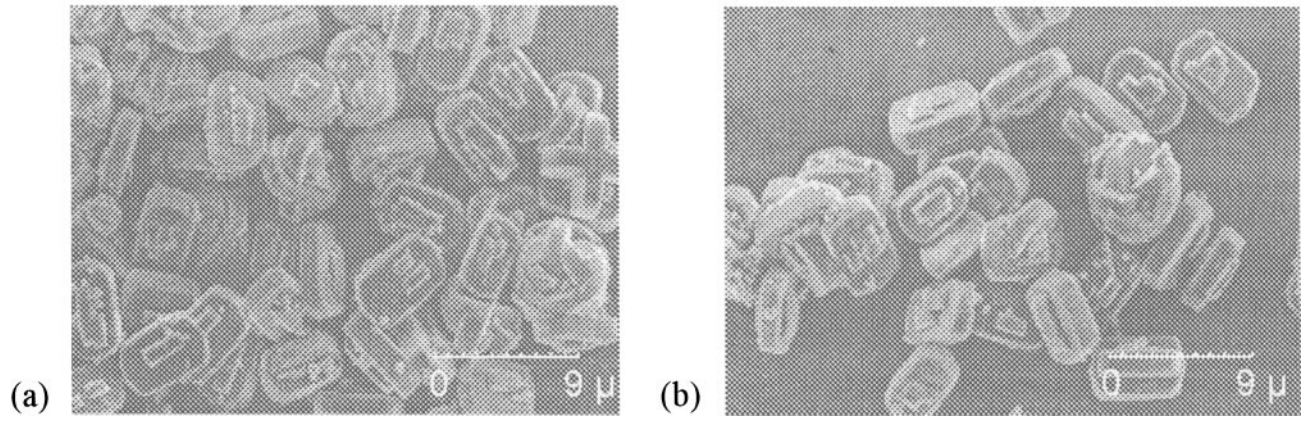

FIG. 1. Scanning electron micrographs of the "large" H-ZSM-5 sample ($d = 1$–$3\ \mu$m) prior to (a) and after (b) oxalic acid treatment over 3 h.

in the size, i.e., in the length of the diffusion path, was observed. The SEM investigation of the sample with the small crystals led to the same conclusion.

Sorption uptake experiments were performed with sample L at 395 K prior to and after the 1.5-h treatment with oxalic acid to check if this treatment caused any additional obstructions to mass transfer. Similar to earlier investigations (3), *o*-xylene was chosen as a test molecule. The sorption kinetic process occurs on identical time scales in both samples investigated. No significant differences between the samples were found. In both cases Fickian diffusion was the rate-determining uptake process, and there were no indications of surface barriers; i.e., the experimental curves could be described by the solution of Fick's law for spherical adsorbents under appropriate boundary conditions.

The intensity of the signal of the bridging hydroxyl groups in the ^{1}H MAS NMR spectrum remains constant despite the acid modification, thus showing that this treatment has not significantly altered the total (external plus internal) concentration of the active sites. This observation is consistent with the results from the catalytic experiments. In this context, note that the contribution of the small amounts of bridging OH groups on the external surface to the ^{1}H MAS NMR signal is in both cases rather low. As shown in Figs. 2 and 3, oxalic acid treatment for 1.5 and 3 h did not change the disproportionation activity of the zeolite samples, neither those with large crystallites nor those with small crystallites. Previous kinetic studies (17) have shown that EB conversion over H-ZSM-5 occurs (under the applied experimental conditions, i.e., catalyst crystallite size and reaction temperature) without diffusion limitations in the interior of the zeolite. Thus, the reaction rate essentially reflects the concentration of the internal acidic sites. Hence, in agreement with the NMR results the constancy of the disproportionation activity confirms that treatment with oxalic acid has not measurably influenced the number of active sites (see above).

In summary, it follows from the above experimental results that oxalic acid treatment did not alter any of the parameters, i.e., k^0 (intrinsic catalytic activity), D (diffusion coefficient of the "slow reactant"), or r (length of the diffusion path), which would affect the *para* selectivity of the catalysts according to model II (see Eq. [3]). Thus, if isomerization model II were valid, the contents of the *p*-DEB over the nontreated and treated catalyst samples should be the same for both samples of different crystallite size.

If, on the other hand, the isomerization of DEB occurred exclusively on the outer surface (model I), then over the acid-treated H-ZSM-5 samples which, compared with the nontreated catalysts, exhibited the same crystal size and disproportionation activity but reduced concentration of the external active sites (cf. Table 1), a lower rate of the secondary isomerization (Eq. [2]) and a higher *para* selectivity would be expected. Moreover, this effect should be stronger for the catalyst with smaller crystallites.

Now, the catalytic experiments provide evidence that there is no difference in the *para* contents of the DEB product prior to and after acid treatment for 1.5 and 3.0 h (see Figs. 4 and 5). This holds for both catalysts of different crystal dimensions and contradicts model I (isomerization only

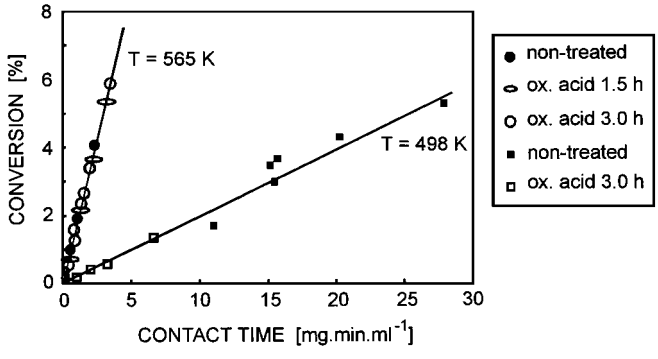

FIG. 2. Conversion of ethylbenzene at 498 and 565 K as a function of contact time, W/F, over H-ZSM-5 catalyst ($d = 1$–$3\ \mu$m) prior to (●, ■) and after (○, ⬭, □) oxalic acid treatment for 1.5 h (ox. acid 1.5 h) and 3.0 h (ox. acid 3.0 h). W = mass of the dry catalyst, F = total flow of EB and helium at 101 kPa total pressure and 1.33 kPa partial pressure of EB.

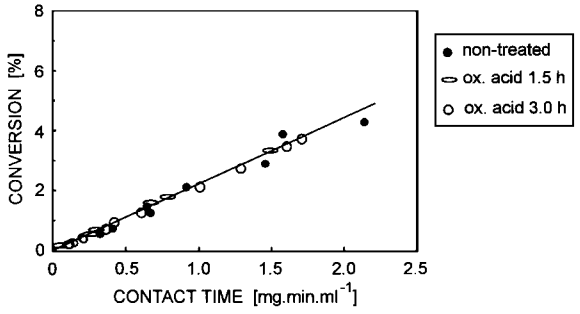

FIG. 3. Conversion of ethylbenzene at 565 K as a function of contact time, W/F, over H-ZSM-5 catalyst ($d = 0.02$–0.05 μm) prior to (●) and after (○, ⬭) oxalic acid treatment for 1.5 h (ox. acid 1.5 h) and 3.0 h (ox. acid 3.0 h). W = mass of the dry catalyst, F = total flow of EB and helium at 101 kPa total pressure and 1.33 kPa partial pressure of EB.

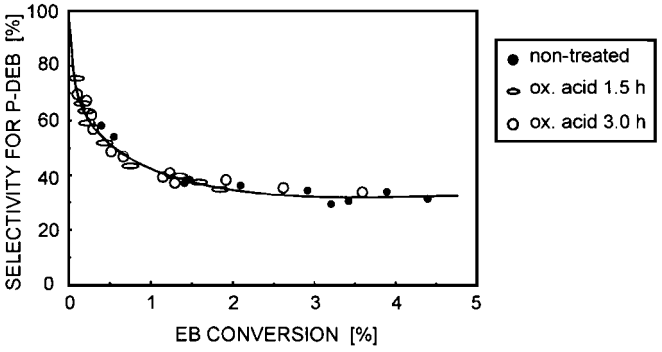

FIG. 5. Selectivity for the *para* isomer of the product diethylbenzene in the EB disproportionation over catalyst H-ZSM-5 ($d = 0.02$–0.05 μm) prior to (●) and after (○, ⬭) oxalic acid treatment for 1.5 h (ox. acid 1.5 h) and 3.0 h (ox. acid 3.0 h). Reaction temperature = 565 K.

on the external surface) but is consistent with model II. Therefore, it appears that the isomerization of DEB proceeds almost exclusively inside the zeolite pores of H-ZSM-5 corresponding to the much higher density of active sites as compared with the external surface, and the *para*-selective features of the catalyst can be understood from an interplay of catalytic reaction and mass transfer. This was confirmed by the results of the subsequent *in situ* IR investigation of the sorption of the pure DEB isomers in H-ZSM-5 zeolite (see below).

2. *In Situ IR Spectroscopic Study of the Adsorption Behavior of DEB Isomers over H-ZSM-5 Zeolite*

The sorption of pure DEB isomers from the gas phase was studied over two H-ZSM-5 samples with crystal diameters of 0.02–0.05 and 2 μm. Additionally, analogous experiments were carried out over the catalytically inactive Na-Y zeolite. The IR spectra of the single sorbates obtained with this sorbent served as a reference to check for possible conversion of the pure substances during sorption into the H-ZSM-5 samples.

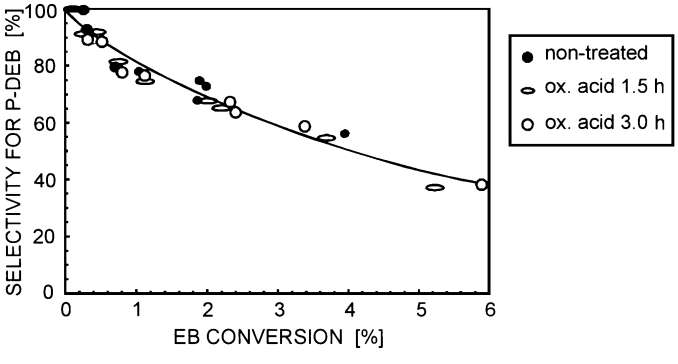

FIG. 4. Selectivity for the *para* isomer of the product diethylbenzene in the EB disproportionation over catalyst H-ZSM-5 ($d = 1$–3 μm) prior to (●) and after (○, ⬭) oxalic acid treatment for 1.5 h (ox. acid 1.5 h) and 3.0 h (ox. acid 3.0 h). Reaction temperature = 565 K.

The two zeolite specimens were exposed to *o*-DEB (partial pressure, 12–61 Pa) at two temperatures, viz. 359 and 522 K. The IR spectra of both sorbents did not change after exposing them to the sorbate over more than 20 h. This shows that *o*-DEB cannot enter the pore system of H-ZSM-5 under the experimental conditions applied. Similar results were reported by Schumacher and Karge (21) and Karge *et al.* (34). These authors studied the sorption of the DEB isomers over H-ZSM-5 samples with larger crystallites and at lower temperatures compared with this investigation.

The two H-ZSM-5 sorbents were exposed to pure *p*-DEB and *m*-DEB under the same conditions as with the *ortho* isomer (see above). In contrast to the *ortho* isomer, *p*-DEB and *m*-DEB were reversibly sorbed into the zeolite. The IR spectra obtained during the uptake experiments with pure *m*-DEB and *p*-DEB at 359 K over H-ZSM-5 are very similar to the corresponding spectra recorded over the catalytically inactive Na-Y (Fig. 6). This indicates that no or very low conversion of the sorbates occurred. Analysis of the spectra of *m*- and *p*-DEB sorbed in H-ZSM-5 at a higher temperature (522 K), however, provides evidence for an isomerization occurring during the sorption. Thus, the IR

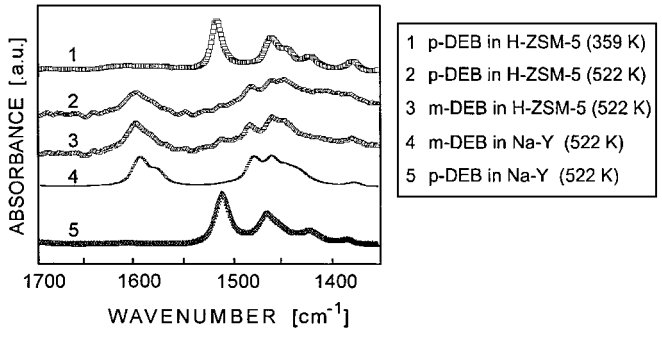

FIG. 6. IR spectra after contacting pure *p*-DEB or *m*-DEB with H-ZSM-5 ($d = 2$ μm) at 359 or 522 K and with Na-Y at 522 K.

spectra obtained after contacting for a few minutes the H-ZSM-5 zeolite with *m*-DEB or *p*-DEB at 522 K are very similar. Both spectra exhibit the characteristic bands of the two pure substances, but those that are typical of the *meta* isomer are more intense (Fig. 6). The higher concentration of *m*-DEB can be readily accounted for by thermodynamic considerations. The equilibrium composition of the DEBs expected at this temperature is as follows: 31% *p*-DEB, 54% *m*-DEB, and 15% *o*-DEB (35). The fact that, irrespective of whether pure *m*-DEB or *p*-DEB is sorbed from the gas phase into H-ZSM-5, the same composition of the sorbate phase in the zeolite pores is observed, shows clearly that DEB isomerization (Eq. [2]) occurs in the interior of this zeolite. Thus, the results from the sorption studies confirm the conclusions derived from the catalytic experiments.

CONCLUSIONS

1. The study of the sorption of *o*-DEB over H-ZSM-5 samples with mean crystallite dimensions equal to or larger than 0.02 μm at sorption temperatures between 359 and 522 K has shown that this sorbate cannot enter the pore system of H-ZSM-5. At variance, *m*-DEB and *p*-DEB are reversibly sorbed into H-ZSM-5 in the temperature range examined.

2. In contrast to several reports in the literature, the isomerization of *p*-DEB to *m*-DEB in the interior of H-ZSM-5 crystallites is possible and occurs mainly there because of the higher concentration of active Brønsted sites inside the crystallites compared with that on the external surface. This was shown by (i) the investigation of the effect of the selective deactivation of the outer crystallite surface on *p*-DEB content of the product of the EB disproportionation over H-ZSM-5, and (ii) the *in situ* IR study of the sorption of pure DEB isomers into H-ZSM-5.

REFERENCES

1. Kaeding, W. W., Chu, C., Young, L. B., Weinstein, B., and Butter, S. A., *J. Catal.* **67**, 159 (1981).
2. Young, L. B., Butter, S. A., and Kaeding, W. W., *J. Catal.* **76**, 418 (1982).
3. Olson, D. H., and Haag, W. O., *Am. Chem. Soc. Symp. Ser.* **248**, 275 (1984).
4. Haag, W. O., and Chen, N. Y., *in* "Catalyst Design" (L. L. Hegedus, Ed.), p. 163. Wiley, New York, 1987.
5. Sulikowski, B., and Klinowski, J., *Z. Phys. Chem.* **177**, 511 (1992).
6. Kürschner, U., Jerschkewitz, H. G., Schreier, E., and Völter, J., *Appl. Catal.* **52**, 167 (1990).
7. Vinek, H., and Lercher, J. A., *J. Mol. Catal.* **64**, 23 (1991).
8. Mirth, G., and Lercher, J. A., *J. Catal.* **132**, 244 (1991).
9. Mirth, G., Cejka, J., and Lercher, J. A., *J. Catal.* **139**, 24 (1991).
10. Mirth, G., Cejka, J., Nusterer, E., and Lercher, J. A., *in* "Proceedings of International Symposium on Zeolites and Microporous Materials: Zeolites and Microporous Crystals, Nagoya, Japan, August 22–25, 1993" (T. Hattori and T. Yashima, Eds.). Elsevier, Amsterdam, 1994. *Stud. Surf. Sci. Catal.* **83**, 287 (1994).
11. Bhat, Y. S., Das, J., Rao, K. V., and Halgeri, A. B., *J. Catal.* **159**, 368 (1996).
12. Melson, S., and Schüth, F., *J. Catal.* **170**, 46 (1997).
13. Haag, W. O., and Olson, D. H., U.S. Patent 3,856,871 (1974).
14. Kaeding, W. W., and Butter, S. A., U.S. Patent 3,911,041 (1975).
15. Butter, S. A., and Young, L. B., U.S. Patent 3,965,209 (1976).
16. Kaeding, W. W., and Young, L. B., U.S. Patent 4,034,053 (1977).
17. Arsenova, N., Haag, W. O., and Karge, H. G., *in* "Proceedings, 11th International Zeolite Conference: Progress in Zeolites and Microporous Materials, Seoul, Korea, August 12–17, 1996" (H. Chon, S. K. Ihm, and Y. S. Uh, Eds.). Elsevier, Amsterdam, 1997. *Stud. Surf. Sci. Catal.* **105**, 1293 (1997).
18. Derouane, E. G., *in* "Proceedings of International Symposium: Catalysis by Zeolites, Ecully (Lyon), September 9–11, 1980" (B. Imelik, C. Naccache, Y. Ben Taarit, G. Coudurier, and H. Praliaud, Eds.). Elsevier, Amsterdam, 1980. *Stud. Surf. Sci. Catal.* **5**, 5 (1980).
19. Nayak, V. S., and Riekert, L., *Appl. Catal.* **23**, 403 (1986).
20. Paparatto, G., Moretti, E., Leofanti, G., and Gatti, F., *J. Catal.* **105**, 227 (1987).
21. Schumacher, R., and Karge, H. G., 9. Deutsche Zeolith-Tagung, Halle, Germany, March 3–5, 1997, Po. 66. *Microporous Mesoporous Mater.* **30**, 307 (1999).
22. Weisz, P. B., and Prater, C. D., *Adv. Catal.* **3**, 143 (1954).
23. Haag, W. O., Lago, R. M., and Weisz, P. B., *Faraday Discuss.* **72**, 317 (1982).
24. Engelhardt, G., and Michel, D., "High-Resolution Solid-State NMR of Silicates and Zeolites," pp. 212–213. Wiley, Chichester, 1987.
25. Brunner, E., Beck, K., Koch, M., Pfeifer, H., Staudte, B., and Zscherpel, D., *in* "Proceedings of 10th International Zeolite Conference: Zeolites and Related Microporous Materials: State of the Art 1994, Garmisch-Partenkirchen, Germany, July 17–22, 1994" (J. Weitkamp, H. G. Karge, H. Pfeifer, and W. Hölderich, Eds.). Elsevier, Amsterdam, 1994. *Stud. Surf. Sci. Catal.* **84**, 357 (1994).
26. Briggs, D., and Seah, M. P., "Practical Surface Analysis by Auger and X-Ray Photoelectron Spectroscopy," pp. 511–514. Wiley, Chichester, 1983.
27. Karge, H. G., Ladebeck, J., Sarbak, Z., and Hatada, K., *Zeolites* **2**, 94 (1982).
28. Schumacher, R., Ehrhardt, K., and Karge, H. G., *Langmuir* **15**, 3965 (1999).
29. Karge, H. G., and Niessen, W., *Catal. Today* **8**, 451 (1991).
30. Colthup, N. B., Daly, L. H., and Wiberly, S. E., "Introduction to Infrared and Raman Spectroscopy," p. 261. Academic Press, New York, 1975.
31. Apelian, M. R., Meeting of The North American Catalysis Society, Snowbird, Utah, June 1995.
32. Apelian, M. R., Fung, A. S., Kennedy, G. J., and Degnan, T. F., *J. Phys. Chem.* **100**, 16577 (1996).
33. Meriaudeau, P., Tuel, A., and Vu, T. T. H., *Catal. Lett.* **61**, 89 (1999).
34. Karge, H. G., Wada, Y., Weitkamp, J., Ernst, S., Girrbach, U., and Beyer, H. K., *in* "Proceedings of 9th Canadian Symposium on Catalysis: Catalysis on the Energy Scene, Quebec, Province of Quebec, September 30–October 3, 1984" (S. Kaliaguine and A. Mahay, Eds.). Elsevier, Amsterdam, 1984. *Stud. Surf. Sci. Catal.* **19**, 101 (1984).
35. Stull, D. R., Westrum, E. F., and Sinke, G. C., "The Chemical Thermodynamics of Organic Compounds," p. 374. Wiley, New York, 1969.